Mathematical Medicine and Biology (2017) **34**, 559–576
doi: 10.1093/imammb/dqw017
Advance Access publication on October 12, 2016

Iontophoretic transdermal drug delivery: a multi-layered approach

GIUSEPPE PONTRELLI* AND MARCO LAURICELLA
Istituto per le Applicazioni del Calcolo, CNR, Rome, Italy
*Corresponding author: Email: giuseppe.pontrelli@gmail.com

AND

JOSÉ A. FERREIRA AND GONÇALO PENA
CMUC, Department of Mathematics, University of Coimbra, Coimbra, Portugal

[Received on 23 December 2015; revised on 10 September 2016; accepted on 13 September 2016]

We present a multi-layer mathematical model to describe the transdermal drug release from an iontophoretic system. The Nernst–Planck equation describes the basic convection–diffusion process, with the electric potential obtained by solving the Laplace's equation. These equations are complemented with suitable interface and boundary conditions in a multi-domain. The stability of the mathematical problem is discussed in different scenarios and a finite-difference method is used to solve the coupled system. Numerical experiments are included to illustrate the drug dynamics under different conditions.

Keywords: drug release; iontophoresis; Nernst–Plank equations; finite-difference methods.

1. Introduction

Traditional transdermal drug delivery (TDD) systems are based on the transport of therapeutic agents across the skin by passive diffusion. Despite being the subject of intense research over the past years, it is still unclear what the exact mechanism of release is and it is often difficult to accurately predict the drug kinetics (Prautnitz *et al.*, 2004; Trommer & Neubert, 2006). Toxicity can arise if an excessive amount of drug is delivered, or if it is released too quickly. On the other hand, if the drug is delivered at a slow rate, or at sufficiently low concentrations, the therapeutic effect vanishes (Prausnitz & Langer, 2008). The success of the TDD is therefore dependent on the amount of drug, rate of release and binding to cell receptors. However, the skin has unique structural and physico-chemical properties which differentiate it from other bio-membranes (Millington & Wilkinson, 1983). The solutes which can be delivered by a transdermal route are limited due to the excellent barrier properties of the stratum corneum, the outermost layer of the epidermis. As a matter of fact, most drugs delivered by conventional systems are constituted by small and highly lipophilic molecules (Pang & Han, 2014). A linear two-layer model has been proposed in Lee *et al.* (1996) to account for drug penetration by intercellular and transcellular pathways in the skin.

To increase the skin's drug transport and overcome the barrier properties of the stratum corneum, innovative technologies have been developed, based on the use of drug transport enhancers. Two main classes of these have been proposed in the literature. The first one is composed of chemical penetration enhancers including surfactants, fatty acids, esters and solvents. These products can have side effects and toxicological implications and appear to be restricted at the present time to experimental strategies. The second group of enhancers, the physical ones, apply an external energy to raise the drug delivery into and across the skin or change the structure of the skin itself and perforate the stratum corneum creating microchannels to facilitate the drug transport (Prausnitz & Langer, 2008; Perumal *et al.*, 2013).

Drug delivery devices based on the application of an external energy source includes electrically assisted systems where the applied potential generates an additional driving force for the drug motion (see Prausnitz, 1996; Becker *et al.*, 2014 and references therein). Among such systems, here we are interested in iontophoretic TDD that several studies have indicated as effective in topical and systemic administration of drugs. It can be used to treat, for instance, dermal analgesia, management of migraine (Ita, 2016) or acute postoperative pain (Power, 2007). More recent applications of iontophoresis have been considered, for instance, in cancer treatment (Komuro *et al.*, 2013; Byrne *et al.*, 2015). In iontophoretic TDD, a charged drug is initially dispersed in a reservoir (or vehicle) which is in contact with the skin, the target tissue. The electric field is generated by a potential of low intensity ($\approx$1 V) and applied over a limited period of time to prevent any skin damage. The iontophoretic transport of an active agent across the skin can be expressed in terms of three independent contributions: passive diffusion due to a chemical gradient, electromigration due to an electric potential gradient and with a minor effect, solute kinetics due to convective solvent flow (electroosmosis) (Pignatello *et al.*, 1996; Gratieri & Kalia, 2013). Moreover, an increased skin permeability arises from changes in the structure of the skin caused by current flow (Pliquett *et al.*, 2000). It should be remarked that chemical reactions are also present in TDD, such as drug degradation, binding and unbinding due to the drug affinity with the polymer chains of the reservoir and/or the target tissue. In this work we are mainly interested in the physical transport and the other effects are neglected.

Mathematical modelling of iontophoretic process allows us to predict drug release from the vehicle and its transport into the target tissue and offers insights into the factors governing drug delivery, such as the duration of applications and their frequency (Kalia *et al.*, 2004). For traditional TDD, the coupling between the diffusion process in the reservoir and in the target tissue has been considered in Barbeiro & Ferreira (2009), Pontrelli & de Monte (2014) and Simon *et al.* (2006). In the majority of TDD models for iontophoretic systems, a constant flux enters the target tissue—composed of one layer only—and the role of the reservoir of finite capacity is neglected (Perumal *et al.*, 2013; Gratieri & Kalia, 2013). In Jaskari *et al.* (2000), the authors consider a two-compartment diffusion model to describe the passive drug evolution while a one layer model is used when the electric field is applied. Tojo has proposed a more general model for iontophoresis incorporating time-dependence, drug binding and metabolism as well as the convective flow term described above (Tojo, 1989). Pikal (1990) developed a relationship between flux enhancement by treating the process as a simple mass transfer through aqueous channels. A strategy to combine mathematical modelling with in-vivo and in-vitro data has been recently proposed in Simon *et al.* (2015). However, none of the above models considers the composite structure of the skin: this aspect has a crucial importance since the drug transport critically relates to the local diffusive properties and, even more importantly, the potential field relies on the layer-dependent electrical conductivities. In this paper we overcome this drawback by considering a coupled diffusion model to describe the drug release from a vehicle in a multi-layered dermal tissue under the action of an electric field. It is well accepted that the skin has an inhomogeneous structure, being composed of several layers with different thickness and physico-chemical-electrical properties. The drug transport in this composite medium is described by Fick's law for the passive diffusion and by the Nernst–Planck equation for the convective transport induced by the potential gradient. It results in a number of coupled convection–diffusion equations defined in a multi-domain, complemented by suitable conditions on the contact surface and on the interfaces between the tissue layers.

The paper is organized as follows. In Section 2 we introduce our vehicle–skin multi-layer physical domain in a general framework. The coupled iontophoretic model is defined in Section 3. The mathematical problem consists of convection–diffusion equations for the drug concentration coupled with the Laplace equation for the electric potential. Due to the material contrast of the layers, we end up with a

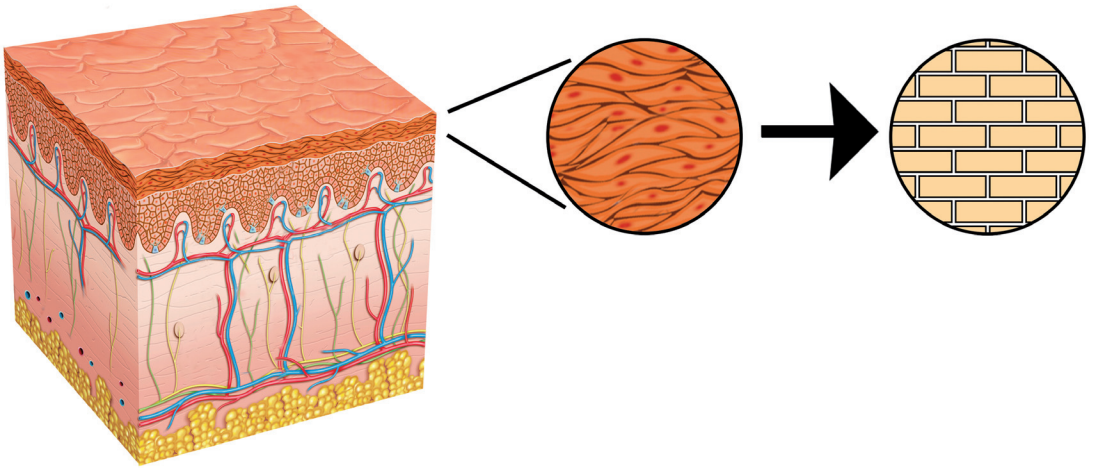

FIG. 1. An anatomic representation of the skin, composed by three main layers: epidermis (approximately 100 μm thick), dermis (between 1 and 3 mm thick, highly vascularized) and a subcutaneous tissue. The epidermis is divided into sub-layers where the stratum corneum (approximately 15 μm thick) is the outermost layer and is the major barrier to the drug migration, being composed of densely packed cells, with a typical 'brick and mortar' structure. Each skin layer, due to its histological composition, and biological function has a different influence in the drug transport mechanism.

stiff mathematical problem. After a suitable nondimensionalization of the initial boundary value problem in Section 4, a finite-difference scheme is described in Section 5 and finally in Section 6 some numerical experiments of TDD are presented and discussed. The complexity of the mathematical system is analysed in the Appendix where two qualitative results concerning its stability are presented.

2. A multi-layer model for the coupled vehicle–skin system

Let us consider a TDD system constituted by (i) a thin layer containing a drug ('the vehicle')[1] and (ii) the skin where the drug is directed to, separated by a protecting film or a semi-permeable membrane. This constitutes a coupled system with an imperfect contact interface for the mass flux between the two media. Because most of the mass dynamics occurs along the direction normal to the skin surface, we restrict our study to a simplified 1D model. In particular, we consider a line crossing the vehicle and the skin, pointing inwards and a Cartesian coordinate x is used along it.

It is well recognized that the skin has a typical composite structure, constituted by a sequence of contiguous layers of different physical properties and thickness, with drug capillary clearance (washout) taking place at the end of it (see Millington & Wilkinson, 1983 for an anatomic and physiological description) (Figs 1 and 2). The vehicle (of thickness ℓ_0) and the skin layers (of thicknesses $\ell_1, \ell_2, \ldots, \ell_n$) are treated as macroscopically homogeneous porous media. Without loss of generality, let us assume that $x_0 = 0$ is the vehicle–skin interface. In a general 1D framework, let us consider a set of intervals

[1]This can be the polymeric matrix of a transdermal patch, or a gel film, or an ointment rub on the skin surface, and acts as the drug reservoir.

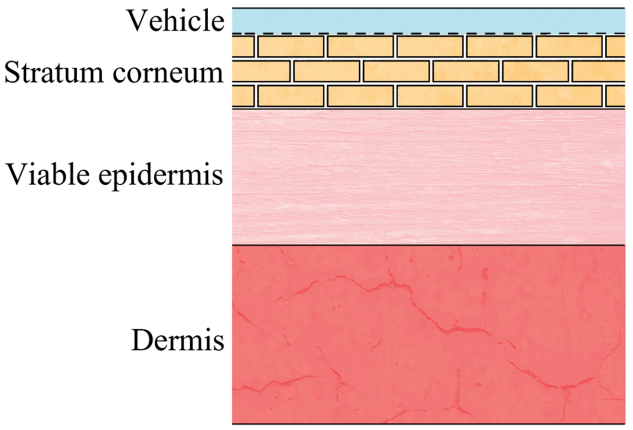

FIG. 2. A schematic section representing the present multi-layered model. A vehicle is applied over the skin surface with an imperfect contact at the vehicle–skin interface (figure not to scale).

$[x_{i-1}, x_i]$, $i = 0, 1, \ldots, n$, having thickness $\ell_i = x_i - x_{i-1}$, modelling the vehicle (layer 0) and the skin (layers $1, 2, \ldots, n$), with $L = \sum_i \ell_i$ the overall skin thickness ($x_n = L$) (Fig. 3).

At the initial time ($t = 0$), the drug is contained only in the vehicle, distributed with maximum concentration C and, subsequently, released into the skin. Here, and throughout this paper, a mass volume-averaged concentration $c_i(x, t)$ (mg cm^{-3}) is considered in each layer ℓ_i. Since the vehicle is made impermeable with a backing protection, no mass flux pass through the boundary surface at $x = x_{-1} = -\ell_0$. Strictly speaking, in a diffusion dominated problem the concentration vanishes asymptotically at infinite distance. However, for computational purposes, the concentration is damped out (within a given tolerance) over a finite distance at a given time. Such a length (sometimes termed as 'penetration distance'), critically depends on the diffusive properties of the layered medium (Pontrelli & de Monte, 2010). At the right end $x = L$ all drug is assumed washed out from capillaries and a sink condition ($c_n = 0$) is imposed.

3. Transdermal iontophoresis

To promote TDD, an electric field is locally applied in the area where the therapeutic agent has to be released ('iontophoresis'): one electrode is placed in contact with the vehicle while the whole body acts as a grounding electrode conductor. To fix ideas, we assume that the drug is positively charged, the anode is at $x = x_{-1}$ and the cathode is at a 'large distance' $x = x_n$ (Fig. 3). Let Ψ_0 and Ψ_1, $\Psi_0 > \Psi_1$, be the corresponding applied potential at the endpoints. By mass conservation, the concentration satisfies the following transport equation:

$$\frac{\partial c_i}{\partial t} + \nabla \cdot J_i = 0 \tag{3.1}$$

and in each layer i the mass flux is defined by the Nernst–Planck flux equation (Gratieri & Kalia, 2013):

$$J_i = -D_i \nabla c_i - u_i c_i \nabla \phi_i, \qquad i = 0, 1, \ldots, n, \tag{3.2}$$

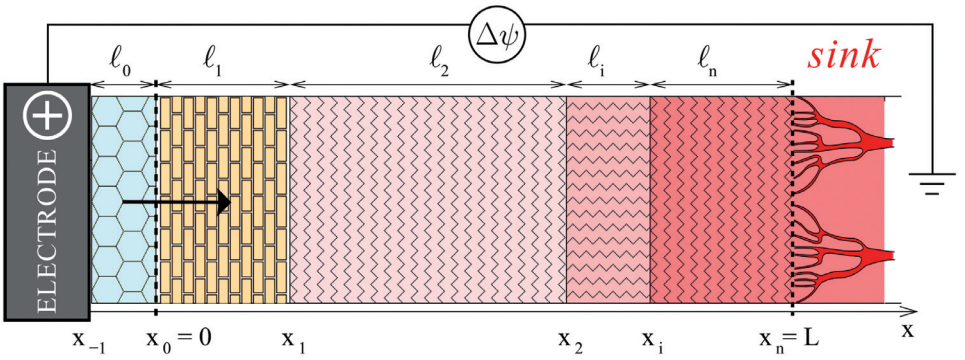

FIG. 3. A diagram sketching a n-layered tissue $(\ell_1, \ell_2, \ldots, \ell_n)$ faced with the vehicle ℓ_0. The 1D model is defined along the line normal to the skin surface and extends with a sequence of n contiguous layers from the vehicle interface $x_0 = 0$ up to the skin bound $x_n = L$, where capillaries sweep the drug away to the systemic circulation (sink). In iontophoresis, a difference of potential $\Delta\Psi$ is applied to facilitate drug penetration from the vehicle across the tissue's layers (figure not to scale).

where $\phi_i(V)$ is the electric potential in layer i and the convective (electroosmotic) term is omitted. Equation (3.2) is the generalized Fick's first law with an additional driving force which is proportional to the electric field. The ith electric mobility is related to the diffusivity coefficient through the Einstein relation:

$$u_i = \frac{D_i z F}{RT}, \qquad i = 0, 1, \ldots, n \tag{3.3}$$

($\mathrm{cm}^2\,\mathrm{V}^{-1}\,\mathrm{s}^{-1}$), where z is the ion valence, F the Faraday constant, R the gas constant, T the absolute temperature. The boundary conditions are

$$J_0 = 0 \qquad \text{at} \quad x = x_{-1} = -\ell_0 \qquad \text{(impermeable backing)}, \tag{3.4}$$

$$c_n = 0 \qquad \text{at} \quad x = x_n = L \qquad \text{(sink condition due to the capillary washout)}. \tag{3.5}$$

The last condition arises because, in deep skin, drug is uptaken by the capillary network and is lost in the systemic circulation: we refer to this as systemically absorbed (shortly 'absorbed') drug. At $x = 0$ we impose the matching of the total fluxes and that they are proportional to the jump of concentration (Kedem–Katchalsky equation):

$$J_0 = J_1 = P(c_0 - c_1) \qquad \text{at} \quad x = 0 \tag{3.6}$$

with P ($\mathrm{cm}\,\mathrm{s}^{-1}$) a mass transfer coefficient (includes a drug partitioning and a mass flux resistance). At the other interfaces we assume a perfect contact and continuity of concentrations and fluxes:

$$J_i = J_{i+1} \qquad c_i = c_{i+1} \qquad \text{at} \quad x = x_i, \qquad i = 1, 2, \ldots, n-1. \tag{3.7}$$

The initial conditions are set as:

$$c_0(x, 0) = C, \qquad c_i(x, 0) = 0 \qquad i = 1, 2, \ldots, n. \tag{3.8}$$

Energy estimates and upper bounds for the initial boundary value problem (3.1)–(3.8) are given in the Appendix A.

3.1 *The electric potential field*

To solve equations (3.1)–(3.3), in some cases the potential ϕ is assigned, but in this multi-layer system we derive it by the continuity equation for the electrical charge:

$$\frac{\partial \rho_i}{\partial t} + \nabla \cdot \mathcal{J}_i = 0 \tag{3.9}$$

with ρ_i is the local charge density and $\mathcal{J}_i$ the electric current density. Because the steady state electric field is established at a time scale much shorter than that associated with the mass diffusion process, the transient effects can safely be neglected. At the steady state, by the Ohm's law relating current density $\mathcal{J}_i$ to the potential ϕ_i, equation (3.9) reduces to:

$$\nabla \cdot (\sigma_i \nabla \phi_i) = 0 \tag{3.10}$$

with $\sigma_i(\Omega^{-1}\,\mathrm{cm}^{-1})$ the electrical conductivity in the layer i (Becker *et al.*, 2014), and

$$\phi_0 = \Psi_0 \qquad \text{at} \quad x = x_{-1}, \tag{3.11}$$

$$\phi_n = \Psi_1 \qquad \text{at} \quad x = x_n. \tag{3.12}$$

At the interfaces we assume an electrically perfect contact and we have continuity of potential and fluxes:

$$-\sigma_i \nabla \phi_i = -\sigma_{i+1} \nabla \phi_{i+1} \qquad \phi_i = \phi_{i+1} \qquad \text{at} \quad x = x_i \qquad i = 0, 1, \ldots, n-1. \tag{3.13}$$

It is straightforward to verify that the general solution of the problem (3.10)–(3.13) is

$$\phi_i(x) = a_i x + b_i \qquad i = 0, 1, \ldots, n, \tag{3.14}$$

where expressions for $a_i(\mathrm{V\,cm}^{-1})$ and $b_i(\mathrm{V})$ are computed through the conditions (3.11)–(3.13) (see section 6).

4. Nondimensional equations

Before solving the differential problem, all the variables, the parameters and the equations are now normalized to get easily computable nondimensional quantities as follows:

$$\begin{aligned}
&\bar{x} = \frac{x}{L} && \bar{t} = \frac{D_{\max}}{L^2} t && \bar{c}_i = \frac{c_i}{C}, \\
&\gamma_i = \frac{D_i}{D_{\max}} && \Pi = \frac{PL}{D_{\max}} && \delta = \frac{\ell_0}{L}, \\
&\bar{\phi}_i = \frac{Fz}{RT} \phi_i && \bar{a}_i = \frac{Fz}{RT} L\, a_i && \bar{b}_i = \frac{Fz}{RT} b_i,
\end{aligned} \tag{4.1}$$

where the subscript max denotes the maximum value across the $n+1$ layers.[2] By omitting the bar for simplicity, the 1D nondimensional Nernst–Planck equations (3.1) and (3.2) become:

$$\frac{\partial c_i}{\partial t} = \gamma_i \frac{\partial^2 c_i}{\partial x^2} + \gamma_i \left(\frac{\partial c_i}{\partial x}\frac{\partial \phi_i}{\partial x} + c_i \frac{\partial^2 \phi_i}{\partial x^2} \right) = \gamma_i \frac{\partial^2 c_i}{\partial x^2} + \gamma_i a_i \frac{\partial c_i}{\partial x} \qquad i = 0, 1, \ldots, n \tag{4.2}$$

(cf. with (3.14)). The above equations are supplemented by the following boundary/interface conditions:

$$J_0 = -\gamma_0 \left(\frac{\partial c_0}{\partial x} + a_0 c_0 \right) = 0 \qquad \text{at} \quad x = -\delta, \tag{4.3}$$

$$\begin{aligned} &J_0 = -\gamma_0 \left(\frac{\partial c_0}{\partial x} + a_0 c_0 \right) = -\gamma_1 \left(\frac{\partial c_1}{\partial x} + a_1 c_1 \right) = J_1 \\ &J_0 = -\gamma_0 \left(\frac{\partial c_0}{\partial x} + a_0 c_0 \right) = \Pi (c_0 - c_1) \qquad \text{at} \quad x = 0, \end{aligned} \tag{4.4}$$

$$\begin{aligned} &J_i = -\gamma_i \left(\frac{\partial c_i}{\partial x} + a_i c_i \right) = -\gamma_{i+1} \left(\frac{\partial c_{i+1}}{\partial x} + a_{i+1} c_{i+1} \right) = J_{i+1} \\ &c_i = c_{i+1} \qquad i = 1, \ldots, n-1 \qquad \text{at} \quad x = x_i, \end{aligned} \tag{4.5}$$

$$c_n = 0 \qquad \text{at} \quad x = 1, \tag{4.6}$$

and initial conditions:

$$c_0(x, 0) = 1 \qquad c_i(x, 0) = 0 \qquad i = 1, 2, \ldots, n. \tag{4.7}$$

5. Numerical solution

Although a semi-analytic treatment is possible in multi-layered diffusion problems (Pontrelli & de Monte, 2010), we proceed to solve the nondimensional system of equations (4.2)–(4.6) numerically. Let us subdivide the interval $(-\delta, 0)$ into $N_0 + 1$ equispaced grid nodes $x_0^j = (j - N_0)\, h_0, \quad j = 0, 1, \ldots, N_0$ and the ith interval $[x_i, x_{i+1}]$ with $N_i + 1$ equispaced points $x_i^j = j\, h_i, \quad j = 0, 1, \ldots, N_i$. Here, $h_0, h_1, h_2, \ldots, h_n$ represent the spacing in the vehicle (layer 0) and skin (layers $i = 1, 2, \ldots, n$), respectively.[3] In each layer, we approximate the diffusive terms by considering a standard finite-difference of the second derivative

[2] The nondimensional quantity $\dfrac{Fz\phi}{RT} = \dfrac{u\phi}{D} = \dfrac{u \nabla \phi L}{D} = \dfrac{[\text{velocity}] \cdot [\text{length}]}{[\text{diffusivity}]}$ measures the relative strength of electrical driven convective to diffusive forces and corresponds to the Péclet number in fluid dynamics problems.

[3] In the following, the subscript i refers to the layer, the superscript j denotes the approximated value of the concentrations at x_i^j.

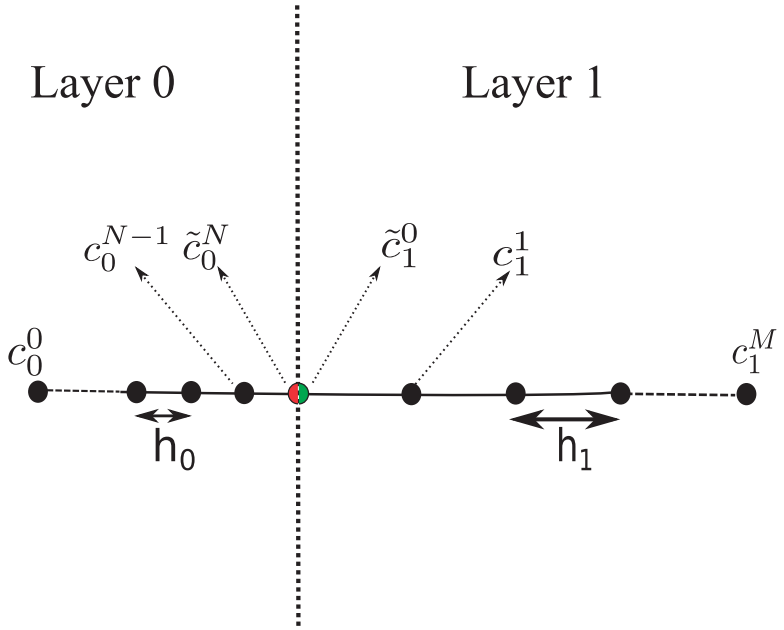

FIG. 4. Schematic illustration of grid nodes in the first two layers and the vehicle-skin interface points (left red and right green). Due to the material contrast, the concentration is not continuous there and the left and right values are computed a posteriori as a linear combination of the neighbouring grid points (equations (5.4) and (5.5)). At the other skin interfaces a single concentration value occurs.

and centred first derivative at internal nodes x_j:

$$\left.\frac{\partial c_i}{\partial x}\right|_{x_j} \simeq \frac{c_i^{j+1} - c_i^{j-1}}{2h_i},$$
$$\left.\frac{\partial^2 c_i}{\partial x^2}\right|_{x_j} \simeq \frac{c_i^{j-1} - 2c_i^j + c_i^{j+1}}{h_i^2} \qquad j = 1, \ldots, N_i - 1 \qquad i = 0, 1, \ldots, n. \tag{5.1}$$

5.1 *Treatment of the interface* $x = 0$

At the interface $x = 0$, we potentially have a discontinuity in concentration and two possibly different values, say $\tilde{c}_0^N$ and $\tilde{c}_1^0$ (the tilde accent indicates these special points), each for each interface side, need to be determined (Fig. 4).

No derivative can be computed across the interface $x = 0$, due to a possible discontinuity and approximations (5.1) no longer apply. An alternative procedure is needed in equation (5.1) to get $\tilde{c}_0^N$ for $j = N_0 - 1$ and $\tilde{c}_1^0$ for $j = 1$. Their values are related through the interface conditions (4.4):

$$-\gamma_0 \left(\frac{\partial \tilde{c}_0^N}{\partial x} + a_0 \tilde{c}_0^N \right) = -\gamma_1 \left(\frac{\partial \tilde{c}_1^0}{\partial x} + a_1 \tilde{c}_1^0 \right),$$
$$-\gamma_0 \left(\frac{\partial \tilde{c}_0^N}{\partial x} + a_0 \tilde{c}_0^N \right) = \Pi(\tilde{c}_0^N - \tilde{c}_1^0). \tag{5.2}$$

Following the approach described by Hickson *et al.* (2011), we take a Taylor series expansion for $c_0^{N-2}, c_0^{N-1}, c_1^1, c_1^2$ and arrive at:

$$\begin{aligned}
c_0^{N-1} &\approx \tilde{c}_0^N - h_0 \frac{\partial \tilde{c}_0^N}{\partial x} + \frac{h_0^2}{2} \frac{\partial^2 \tilde{c}_0^N}{\partial x^2}, \\
c_0^{N-2} &\approx \tilde{c}_0^N - 2h_0 \frac{\partial \tilde{c}_0^N}{\partial x} + 2h_0^2 \frac{\partial^2 \tilde{c}_0^N}{\partial x^2}, \\
c_1^1 &\approx \tilde{c}_1^0 + h_1 \frac{\partial \tilde{c}_1^0}{\partial x} + \frac{h_1^2}{2} \frac{\partial^2 \tilde{c}_1^0}{\partial x^2}, \\
c_1^2 &\approx \tilde{c}_1^0 + 2h_1 \frac{\partial \tilde{c}_1^0}{\partial x} + 2h_1^2 \frac{\partial^2 \tilde{c}_1^0}{\partial x^2}.
\end{aligned} \tag{5.3}$$

The two equations (5.2) and the four equations (5.3) form an algebraic system of six equations that allow to express $\tilde{c}_0^N, \tilde{c}_1^0$ and their first and second derivatives as a linear combination of the neighbouring values. Using symbolic calculus we obtain:

$$\tilde{c}_0^N = \frac{[\gamma_0\gamma_1(3 - 2ah_1) + 2\Pi\gamma_0 h_1](c_0^{N-2} - 4c_0^{N-1}) + 2\gamma_1 h_0 \Pi(c_1^2 - 4c_1^1)}{Q}, \tag{5.4}$$

$$\tilde{c}_1^0 = \frac{[\gamma_0\gamma_1(3 + 2a_0h_0) + 2\Pi\gamma_1 h_0](c_1^2 - 4c_1^1) + 2\gamma_0 h_1 \Pi(c_0^{N-2} - 4c_0^{N-1})}{Q}, \tag{5.5}$$

where $Q = 2\gamma_1 h_0 \Pi(2ah_1 - 3) + \gamma_0(2a_0h_0 + 3)(2a\gamma_1 h_1 - 3\gamma_1 - 2h_1\Pi)$.

After spatial discretization, the system of PDEs reduces to a system of nonlinear ordinary differential equations (ODEs) of the form:

$$\frac{dY}{dt} = A(Y), \tag{5.6}$$

where $Y = (c_0^0, \ldots, c_0^{N-1}, c_1^1, \ldots, c_1^{N_1}, \ldots, c_n^0, \ldots c_n^{N_n})^T$ and $A(Y)$ contains the coupled $N_0 + N_1 + \cdots + N_n$ discretized equations (4.2). The system (5.6) is solved by the routine ode15s of `Matlab` based on a Runge–Kutta type method with backward differentiation formulas, and an adaptive time step. The interface drug concentrations $\tilde{c}_0^N, \tilde{c}_1^0$ are computed a posteriori through equations (5.4) and (5.5).

6. Results and discussion

A common difficulty in simulating physiological processes, in particular TDD, is the identification of reliable estimates of the model parameters. Experiments of TDD are impossible or prohibitively expensive in vivo and the only available source are lacking and incomplete data from literature. The drug delivery problem depends on a large number of constants, each of them varies in a finite range, with a variety of combinations and limiting cases. Furthermore, these parameters can be influenced by body delivering site, patient age and individual variability, being subject to a high degree of uncertainty. They cannot be chosen independently from each other and there is a compatibility condition among them.

TABLE 1 *The parameters used in the simulations for the vehicle and the three skin layers*

—	Vehicle (0)	Stratum corneum (1)	Viable epidermis (2)	Dermis (3)
$l_i = x_i - x_{i-1}$ (cm)	0.01	$1.75 \cdot 10^{-3}$	$3.5 \cdot 10^{-3}$	0.11
D_i ($\mathrm{cm^2 s^{-1}}$)	10^{-4}	10^{-10}	10^{-7}	10^{-7}
σ_i ($\Omega^{-1}\,\mathrm{cm^{-1}}$)	$1.5 \cdot 10^{-2}$	10^{-7}	10^{-4}	10^{-4}

Here, the skin is assumed to be composed of three main layers, say the stratum corneum, the viable epidermis and the dermis with respective model parameters given in Table 1. For the diffusion and electrical transport properties, the viable epidermis is usually treated as an aqueous tissue nearly equivalent to the dermis (Nitsche & Kasting, 2013) . In the absence of direct measurements, indirect data are inferred from previous studies in the literature (Prausnitz, 1996; Millington & Wilkinson, 1983; Becker, 2012). Diffusivities critically depend on the kind and size of the transported molecules and are affected by a high degree of uncertainty. The vehicle–skin permeability parameter is estimated as $P = 10^{-5}\mathrm{cm\ s^{-1}}$, following analogous studies in biological tissues (Pontrelli & de Monte, 2010).

The coefficients of potential ϕ_i in equation (3.14) have the following expressions:

$$
\begin{aligned}
a_0 &= -\frac{\Delta\Psi\sigma_1\sigma_2\sigma_3}{G},\\
b_0 &= \frac{l_0\Psi_1\sigma_1\sigma_2\sigma_3 + l_1\Psi_0\sigma_0\sigma_3(\sigma_2-\sigma_1) + l_2\Psi_0\sigma_0\sigma_1(\sigma_3-\sigma_2) + l_3\Psi_0\sigma_0\sigma_1\sigma_2}{G},\\
a_1 &= -\frac{\Delta\Psi\sigma_0\sigma_2\sigma_3}{G}\\
b_1 &= \frac{l_0\Psi_1\sigma_1\sigma_2\sigma_3 + l_1\Psi_0\sigma_0\sigma_3(\sigma_2-\sigma_1) + l_2\Psi_0\sigma_0\sigma_1(\sigma_3-\sigma_2) + l_3\Psi_0\sigma_0\sigma_1\sigma_2}{G} = b_0,\\
a_2 &= -\frac{\Delta\Psi\sigma_0\sigma_1\sigma_3}{G},\\
b_2 &= \frac{l_0\Psi_1\sigma_1\sigma_2\sigma_3 + l_1\Psi_1\sigma_0\sigma_3(\sigma_2-\sigma_1) + l_2\Psi_0\sigma_0\sigma_1(\sigma_3-\sigma_2) + l_3\Psi_0\sigma_0\sigma_1\sigma_2}{G},\\
a_3 &= -\frac{\Delta\Psi\sigma_0\sigma_1\sigma_2}{G},\\
b_3 &= \frac{l_0\Psi_1\sigma_1\sigma_2\sigma_3 + l_1\Psi_1\sigma_0\sigma_3(\sigma_2-\sigma_1) + l_2\Psi_1\sigma_0\sigma_1(\sigma_3-\sigma_2) + l_3\Psi_0\sigma_0\sigma_1\sigma_2}{G},
\end{aligned}
\tag{6.1}
$$

where $G = l_0\sigma_1\sigma_2\sigma_3 + l_1\sigma_0\sigma_3(\sigma_2-\sigma_1) + l_2\sigma_0\sigma_1(\sigma_3-\sigma_2) + l_3\sigma_0\sigma_1\sigma_2$ and $\Delta\Psi = \Psi_0 - \Psi_1$. Note that only the electric potential gradients, a_i, appear in the Nernst–Planck equation and the ratio of the slopes satisfies: $\dfrac{a_i}{a_{i+1}} = \dfrac{\sigma_{i+1}}{\sigma_i}$.

Instead of reproducing the clinical protocols where iontophoresis consists in repeated sessions of 10–20 min, the numerical simulations aim at bringing to extreme values both the potential (up to $\Delta\Psi = 10$ V) and the duration of application (30 min): a current is activated during this period of time and then switched off. In Fig. 5 the concentration profiles are shown before (continuous lines) and after (dashed lines) the current application. The iontophoretic effect is to enhance the stratum corneum permeation, but

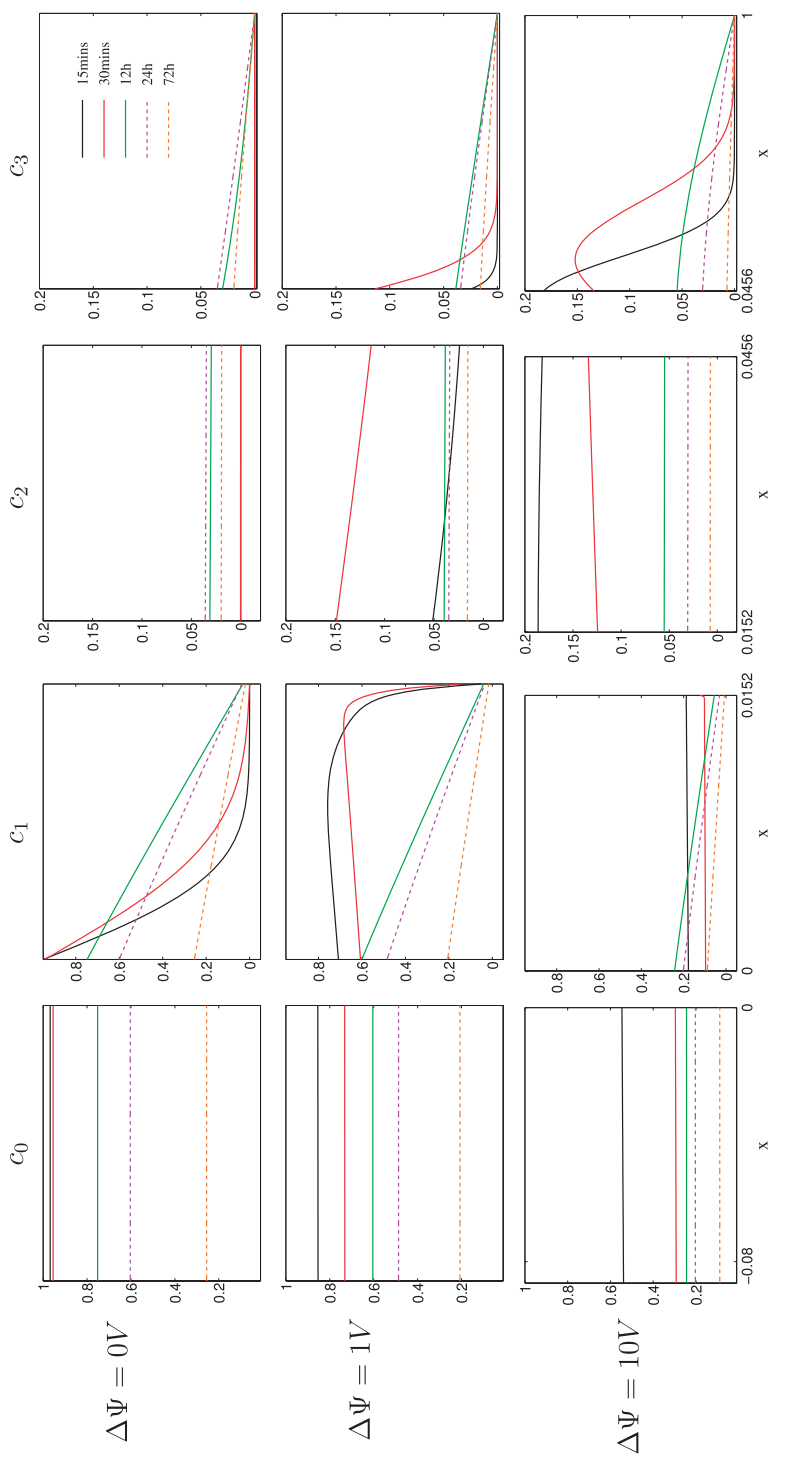

FIG. 5. Profiles of concentration in all layers at five times (continuous lines during current administration, dashed lines after suspension), for three differences of potential. The effect of iontophoresis is to enhance penetration in the stratum corneum, and for higher voltage, even in the deeper layers (simulations based on a uniform mesh size $h_0 = h_1 = h_2 = h_3 = 2 \cdot 10^{-3}$, current switched off after 30 min).

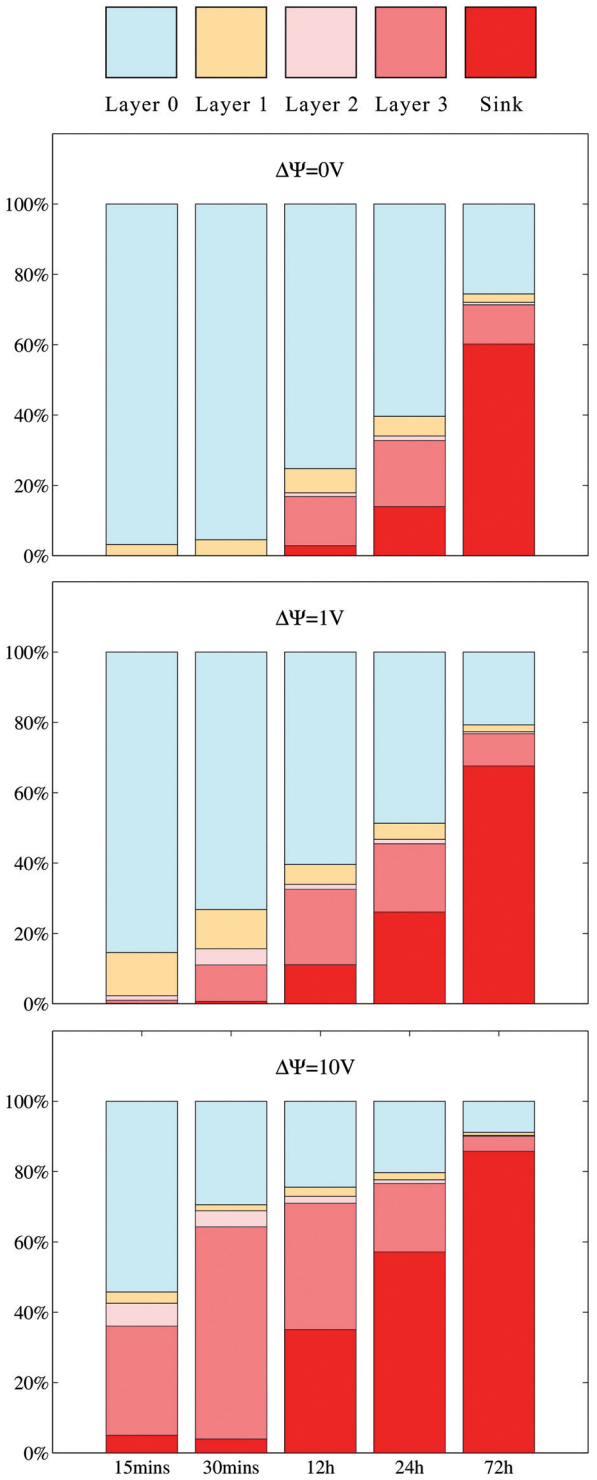

FIG. 6. Distribution of mass in all layers (including the vehicle (layer 0) and the sink) at five times, for three differences of potential. The heights of the rectangles indicate the percentage of mass retained in each layer. A higher current accelerates depletion of the vehicle and enhances drug delivery in stratum corneum and in the deeper skin's layers. At later times most of drug results absorbed at the systemic level (current switched off after 30 min).

appears to be significant in deeper layers only for higher $\Delta\Psi$. No relevant effect is present after current suspension. It is desirable the drug level is maintained over a certain amount to exert its therapeutic effect without exceeding a given threshold to not be toxic.

In Fig. 6 the different distribution of drug mass in all layers is depicted: mass is decreasing in the vehicle, whereas in the other layers it is first increasing, reaches a peak, and asymptotically decreasing, as in other similar drug delivery systems (Pontrelli & de Monte, 2010, 2014). Due to the sink condition at the right end, part of mass is lost via the systemic circulation. By considering this effect, a drug mass conservation holds and the progressive emptying of the vehicle corresponds to the drug replenishment of the other layers—in a cascade sequence—at a rate depending on the electric field (Fig. 6). Again, an augmented transdermal permeation is reported with higher values of the potential: this is more effective during current administration, but prolongs at later times (12–72 h). The transport of a species across skin will be determined by the strength and the duration of the electric field, the concentration and the mobility of all ions in the skin. The desired delivery rate is obtained with a proper choice of the physico-chemical-electrical parameters.

These outcomes provide valuable indications to assess whether and to what extent drug reaches a deeper layer, and to optimize the dose capacity in the vehicle. Therefore, it is possible to identify the conditions that guarantee a more prolonged and uniform release or a localized peaked distribution.

7. Conclusions

Nowadays iontophoretic systems are commonly used in transdermal applications. These systems use an electric field to enhance the release from a drug reservoir and to direct the therapeutic action at the target tissue with a given rate and at desired level. Iontophoresis provides a mechanism to control the transport of hydrophilic and charged agents across the skin, especially for high molecular weight substances such as peptides or proteins which are usually ionized and hardly penetrate the stratum corneum by conventional passive diffusion. Notwithstanding, the effective utilization of electric field-assisted transport for drug delivery across biological membranes requires a deeper understanding of the mechanisms and theories behind the process.

In this paper a multi-layer model is developed to clarify the role of the applied potential, the conductivity of the skin, the drug diffusion and the systemic absorption. The stability of the mathematical problem is discussed within two different scenarios: imperfect and perfect contact between the reservoir and the target tissue. To illustrate the drug dynamics in the composite medium—vehicle and skin layers coupled together—during and after the electric administration, an accurate finite-difference method is proposed. The modelling approach allows the simulation in several experimental setting, including extreme conditions which are not possible in clinical environment. Numerical experiments show how the applied current, along the duration of application, accelerates the depletion of the reservoir, distributes drug levels among the layers, and increases the drug absorption in the deep skin. As in many biological systems, the model suffers from the lack of estimating the several parameters, that are subject to variability and uncertainty. As such, the present TDD model has to be intended as a simple available tool indicating new delivering strategies that guarantee the optimal and localized release for an extended period of time.

Acknowledgements

We are grateful to E. Di Costanzo for many valuable discussions and helpful comments.

Funding

The support of the bilateral project FCT-CNR 2015–2016 is greatly acknowledged. This work was partially supported by the Centre for Mathematics of the University of Coimbra—UID/MAT/00324/2013, funded by the Portuguese Government through FCT/MEC and co-funded by the European Regional Development Fund through the Partnership Agreement PT2020.

References

Barbeiro, S. & Ferreira, J. A. (2009) Coupled vehicle-skin models for drug release. *Comput. Methods Appl. Mech. Eng.*, **198**, 2078–2086.

Becker, S. (2012) Transport modeling of skin electroporation and the thermal behavior of the stratum corneum. *Int. J. Thermal Sci.*, **54**, 48–61.

Becker, S., Zorec, B., Miklavčič, D. & Pavšelj, N. (2014) Transdermal transport pathway creation: electroporation pulse order. *Math. Biosci*., **257**, 60–68.

Byrne, J., Jajja, M., O'Neill, A., Bickford, L. et al., (2015) Local iontophoretic administration of cytotoxic therapies to solid tumors. *Sci. Transl. Med*., **7**, 273.

Gratieri, T. & Kalia, Y. (2013) Mathematical models to describe iontophoretic transport in vitro and in vivo and the effect of current application on the skin barrier. *Adv. Drug Deliv. Rev.*, **65**, 315-329.

Hickson, R. I., Barry, S. I., Mercer, G. N. & Sidhu, H. S. (2011) Finite difference schemes for multilayer diffusion. *Math. Comp. Model*., **54**, 210–220.

Ita, K. (2016) Transdermal iontophoretic drug delivery: advances and challenges. *J. Drug Target.*, **24**, 386–391.

Jaskari, T., Vuorio, M., Kontturi, K., Urtti, A., Manzanares, J. & Hirvonen, J. (2000) Controlled transdermal iontophoresis by ion-exchange fiber. *J. Control. Release*, **67**, 179–190.

Kalia, Y. N., Naik, A., Garrison, J. & Guy, R. H. (2004) Iontophoretic drug delivery. *Adv. Drug Deliv. Rev.* **56**, 619–658.

Komuro, M., Suzuki, K., Kanebako, M., Kawahara, T., Otoi, T., Kitazato, K., Inagi, T., Makino, K., Toi, M. & Terada, H. (2013) Novel iontophoretic administration method for local therapy of breast cancer. *J. Control. Release*, **168**, 298–306.

Lee, A. J., King, J. R. & Rogers, T. G. (1996) A multiple-pathway model for the diffusion of drugs in the skin. *J. Math. Appl. Med. Biol*. **13**, 127–150.

Millington, P. F. & Wilkinson, R. (1983) *Skin*. United Kingdom: Cambridge University Press.

Nitsche, J. M. & Kasting, G. B. (2013) A microscopic multiphase diffusion model of viable epidermis permeability. *Biophys. J.*, **104**, 2307–2320.

Pang, Z. & Han, C. (2014) Review on transdermal drug delivery systems. *J. Pharm. Drug Dev*., **2**, 1–10.

Perumal, O., Murthy, S. & Kalia, Y. (2013) Tuning theory in practice: the development of modern transdermal drug delivery systems and future trends. *Skin Pharm. Physiol.*, **26**, 331–342.

Pignatello, R., Frest, M. & Puglisi, G. (1996) Transdermal drug delivery by iontophoresis. I. Fundamentals and theoretical aspects. *J. Appl. Cosmetol.*, **14**, 59–72.

Pikal, M. (1990) Transport mechanisms in iontophoresis.I. A theoretical model for the effect of electroosmotic flow on flux enhancement in transdermal iontophoresis. *Pharm. Res*., **7**, 118–126.

Pliquett, U. F., Gusbeth, C. A. & Weaver, J. C. (2000) Non-linearity of molecular transport through human skin due to electric stimulus. *J. Control. Release*, **68**, 373–386.

Pontrelli, G. & de Monte, F. (2010) A multi-layer porous wall model for coronary drug-eluting stents. *Int. J. Heat Mass Transf*., **53**, 3629–3637.

Pontrelli, G. & de Monte, F. (2014) A two-phase two-layer model for transdermal drug delivery and percutaneous absorption. *Math. Biosci*., **257**, 96–103.

Power, I. (2007) Fentanyl HCl iontophoretic transdermal system (ITS): clinical application of iontophoretic technology in the management of acute postoperative pain. *Br. J. Anaesth*., **98**, 4–11.

PRAUSNITZ, M. R. (1996) The effects of electric current applied to skin: a review for transdermal drug delivery. *Adv. Drug Deliv. Rev.*, **18**, 395–425.

PRAUSNITZ, M. & LANGER, R. (2008) Transdermal drug delivery. *Nat. Biotechnol.*, **26**, 1261–1268.

PRAUSNITZ, M., MITRAGORI, S. & LANGER, R. (2004) Current status and future potential of transdermal drug delivery. *Nat. Rev. Drug Discov.*, **3**, 115–124.

SIMON, L., OSPINA, J. & ITA, K. (2015) Prediction of in-vivo iontophoretic drug release data from in-vitro experiments – insights from modeling. *Math. Biosci.*, **270**, 106–114.

SIMON, L., WELTNER, A. N., WANG, Y. & MICHNIAK, B. (2006) A parametric study of iontophoretic transdermal drug-delivery systems. *J. Membr. Sci.*, **278**, 124–132.

TOJO, K. (1989) Mathematical model of intophoretic transdermal drug delivery. *J. Chem. Eng. Jpn.*, **22**, 512–518.

TROMMER, H. & NEUBERT, R. (2006) Overcoming the stratum corneum: the modulation of skin penetration. *Skin Pharmacol. Physiol.*, **19**, 106–121.

Appendix A

We now establish some energy estimates of the initial boundary value problem (3.1)–(3.8) in the two cases of finite $P > 0$ (Section A.1) and in the limit case $P \to \infty$ (Section A.2) at interface condition (3.6), that leads to upper bound of total drug masses. These results are used to obtain stability and uniqueness results under a condition on the applied potential and on the diffusivities. We point out that our analysis concerns the global energy as well as the total mass of drug in the whole system, and cannot apply in the single layers.

A.1 *The general case: imperfect contact*

Let $(\cdot,\cdot)_i$ be the usual inner product in $L^2(x_{i-1}, x_i)$ and $\|\cdot\|_i$ the corresponding norm, $i = 0, \ldots, n$. From (3.1) we deduce

$$\sum_{i=0}^{n} \left(\frac{\partial c_i}{\partial t}, c_i \right)_i + \sum_{i=0}^{n} (\nabla \cdot J_i, c_i)_i = 0. \tag{A.1}$$

Combining (A.1) with the boundary conditions (3.4) and (3.5) and the interface conditions (3.6), (3.7) we get

$$\frac{1}{2}\xi'(t) + \sum_{i=0}^{n} D_i \|\nabla c_i\|_i^2 + \sum_{i=0}^{n} (v_i c_i, \nabla c_i)_i = -P\big(c_0(0,t) - c_1(0,t)\big)^2, \tag{A.2}$$

where $v_i = u_i \nabla \phi_i$, is the convective velocity induced by the potential field, and $\xi(t) = \sum_{i=0}^{n} \|c_i(t)\|_i^2$ is the total energy. By the Young inequality we have:

$$(v_i c_i, \nabla c_i)_i \geq -\frac{1}{4\epsilon_i^2} v_i^2 \|c_i\|_i^2 - \epsilon_i^2 \|\nabla c_i\|_i^2,$$

for any $\epsilon_i \neq 0$. Then from (A.2) we get

$$\frac{1}{2}\xi'(t) + \sum_{i=0}^{n}\left(D_i - \epsilon_i^2\right)\|\nabla c_i\|_i^2 - \sum_{i=0}^{n}\frac{v_i^2}{\epsilon_i^2}\|c_i\|_i^2 \leq -P\big(c_0(0,t) - c_1(0,t)\big)^2. \tag{A.3}$$

Taking $\epsilon_i^2 = D_i$ in (A.3) we obtain:

$$\xi'(t) - 2\sum_{i=0}^{n}\frac{v_i^2}{D_i}\|c_i\|_i^2 \leq -2P\big(c_0(0,t) - c_1(0,t)\big)^2. \tag{A.4}$$

Finally, (A.4) leads to

$$\xi(t) \leq e^{\alpha t}\left(\xi(0) - 2P\int_0^t e^{-\alpha s}\big(c_0(0,s) - c_1(0,s)\big)^2 ds\right) \tag{A.5}$$

with $\alpha = 2\max\limits_{i=0,\ldots,n}\dfrac{v_i^2}{D_i}$. The upper bound (A.5) shows that the initial boundary value problem (3.1)–(3.8) is stable for finite t. Through the previous inequality, we prove the uniqueness of the solution as follows: if we assume that in each sub-interval we have at least two solutions c_i and $\tilde{c}_i$ that satisfy the same initial condition, then for $w_i = c_i - \tilde{c}_i$ we have

$$\xi(t) \leq e^{\alpha t}\Big(- 2P\int_0^t e^{-\alpha s}\big(w_0(0,s) - w_1(0,s)\big)^2 ds\Big). \tag{A.6}$$

This means that $\xi(t) \leq 0$ and consequently $c_i = \tilde{c}_i, i = 0,\ldots,n$. The existence of the solution is guaranteed by showing that an analytic solution can be built as a Fourier series, analogously to similar diffusion-convective problems in layered systems (Pontrelli & de Monte, 2014). Let us now define D, v and c as:

$$D(x) = D_i, \qquad v(x) = v_i, \qquad c(x,t) = c_i(x,t), \qquad x \in (x_{i-1}, x_i),\ i = 0,\ldots,n$$

with $(\cdot,\cdot)$ the usual inner product in $L^2(-\ell_0, L)$ and $\|\cdot\|$ the corresponding norm.

The upper bound (A.5) can be used to describe the behaviour of the coupled system for the released mass. Let

$$M_i(t) = \int_{x_{i-1}}^{x_i} c_i(x,t)dx \qquad M(t) = \sum_{i=0}^{n} M_i(t) = \int_{-\ell_0}^{L} c(x,t)dx \tag{A.7}$$

be the mass in the layer i and the total mass, respectively. Using Hölder's inequality, we get:

$$M^2(t) = \left(\int_{-\ell_0}^{L} c(x,t)dx\right)^2 \leq \mathcal{L}\,\xi(t),$$

where $\mathcal{L} = L + \ell_0$ is the total vehicle and skin thickness. Hence, from equation (A.5), we get the following upper bound for the drug mass in the coupled system

$$M(t) \leq \sqrt{\mathcal{L}}e^{\frac{\alpha}{2}t}\left(\xi(0) - 2P\int_0^t e^{-\alpha s}\big(c_0(0,s) - c_1(0,s)\big)^2 ds\right)^{1/2}. \tag{A.8}$$

This estimate shows that the larger is P, the smaller is the upper bound in equation (A.8). The above bound depends on the history of concentration jump at contact interface weighted by controllable quantities such as the applied potential and the media diffusivities.

A.2 *The limit case $P \to \infty$: perfect contact*

We now consider the limit case of $P \to \infty$ in (3.6) , that is when the contact between the vehicle and the target tissue is perfect, and allows the continuity of the concentration in the interface between both media:

$$c_0 = c_1 \qquad \text{at} \quad x = 0. \tag{A.9}$$

Differently from the previous subsection, the regularity of c in $(-\ell_0, L)$ allows the use of the Poincaré inequality. By observing that $\xi(t) = \|c(t)\|^2$, we have:

$$\frac{1}{2}\xi'(t) = -(D\nabla c(t), \nabla c(t)) - (vc(t), \nabla c(t)). \tag{A.10}$$

Being

$$-(vc(t), \nabla c(t)) \leq \max_{i=0,\dots,n} |v_i| \|c(t)\| \|\nabla c(t)\|,$$

and taking into account the following Poincaré inequality $\xi(t) \leq \dfrac{\mathcal{L}^2}{2}\|\nabla c(t)\|^2$, we obtain

$$-(vc(t), \nabla c(t)) \leq \max_{i=0,\dots,n} |v_i| \frac{\mathcal{L}}{\sqrt{2}} \|\nabla c(t)\|^2.$$

Inserting the last upper bound in (A.10) we deduce

$$\xi'(t) \leq \Big(-2 \min_{i=0,\dots,n} D_i + \max_{i=0,\dots,n} |v_i| \sqrt{2}\mathcal{L} \Big) \|\nabla c(t)\|^2. \tag{A.11}$$

If

$$\max_{i=0,\dots,n} \frac{|v_i|}{D_i} \mathcal{L} \leq \sqrt{2} \tag{A.12}$$

by applying the Poincaré inequality in (A.11), we get

$$\xi(t) \leq e^{\beta t} \|c(0)\|^2, \tag{A.13}$$

where

$$\beta = \frac{1}{\mathcal{L}^2} \Big(-2 \min_{i=0,\dots,n} D_i + \max_{i=0,\dots,n} |v_i| \sqrt{2}\mathcal{L} \Big).$$

Under the condition (A.12) we get the mass upper bound:

$$M(t) \leq \sqrt{\mathcal{L}} e^{\beta t} \|c(0)\|. \tag{A.14}$$

From equation (A.14), the exponential decay of the upper bound for the drug mass $M(t)$ results provided that (A.12) holds.